Circulation Research

JOURNAL OF THE AMERICAN HEART ASSOCIATION

American Heart Association®

# Mapping Cardiac Pacemaker Circuits: Methodological Puzzles of the Sinoatrial Node Optical Mapping

Igor R. Efimov, Vadim V. Fedorov, Boyoung Joung and Shien-Fong Lin

*Circ Res.* 2010;106:255-271
doi: 10.1161/CIRCRESAHA.109.209841
*Circulation Research* is published by the American Heart Association, 7272 Greenville Avenue, Dallas, TX 75231

Print ISSN: 0009-7330. Online ISSN: 1524-4571

This Review is part of a new thematic series on **Mechanisms of Pacemaking in the Heart**, which includes the following articles:
Be Still, My Beating Heart—Never! [2010;106:238–239]
Development of the Pacemaker Tissues of the Heart [2010;106:240–254]

Mapping Cardiac Pacemaker Circuits: Methodological Puzzles of the Sinoatrial Node Optical Mapping

The Role of the Funny Current in Pacemaker Activity
$Ca^{2+}$ Cycling in the Mechanism of Pacemaking
Cardiac Pacemaking: Historical Overview and Future Directions

***Denis Noble, Guest Editor, and Brian O'Rourke, Editor***

# Mapping Cardiac Pacemaker Circuits

## Methodological Puzzles of the Sinoatrial Node Optical Mapping

Igor R. Efimov, Vadim V. Fedorov, Boyoung Joung, Shien-Fong Lin

**Abstract: Historically, milestones in science are usually associated with methodological breakthroughs. Likewise, the advent of electrocardiography, microelectrode recordings and more recently optical mapping have ushered in new periods of significance of advancement in elucidating basic mechanisms in cardiac electrophysiology. As with any novel technique, however, data interpretation is challenging and should be approached with caution, as it cannot be simply extrapolated from previously used methodologies and with experience and time eventually becomes validated. A good example of this is the use of optical mapping in the sinoatrial node (SAN): when microelectrode and optical recordings are obtained from the same site in myocardium, significantly different results may be noted with respect to signal morphology and as a result have to be interpreted by a different set of principles. Given the rapid spread of the use of optical mapping, careful evaluation must be made in terms of methodology with respect to interpretation of data gathered by optical sensors from fluorescent potential-sensitive dyes. Different interpretations of experimental data may lead to different mechanistic conclusions. This review attempts to address the origin and interpretation of the "double component" morphology in the optical action potentials obtained from the SAN region. One view is that these 2 components represent distinctive signals from the SAN and atrial cells and can be fully separated with signal processing. A second view is that the first component preceding the phase 0 activation represents the membrane currents and intracellular calcium transients induced diastolic depolarization from the SAN. Although the consensus from both groups is that ionic mechanisms, namely the joint action of the membrane and calcium automaticity, are important in the SAN function, it is unresolved whether the double-component originates from the recording methodology or represents the underlying physiology. This overview aims to advance a common understanding of the basic principles of optical mapping in complex 3D anatomic structures. (*Circ Res*. 2010;106:255-271.)**

**Key Words:** sinoatrial node ■ optical mapping ■ calcium ■ sinoatrial exit block

During the last 20 years, optical mapping has significantly advanced cardiac electrophysiology research. However, interpretation of optical signals from 3D anatomic structures has been a subject of debate. This overview presents two points of view in relation to optical mapping of the canine sinus node.

## Part I. By Vadim V. Fedorov and Igor R. Efimov

The history of cardiac physiology is best exemplified in the discovery and investigation of the sinoatrial node (SAN). It was discovered by Flack in the Keith laboratory in 1907,[1] following guidance from the precise morphological description of the atrioventricular node, which was

Original received July 14, 2009; resubmission received September 22, 2009; revised resubmission received October 28, 2009; accepted November 3, 2009.
From the Department of Biomedical Engineering (I.R.E., V.V.F.), Washington University in St Louis, Mo; and Krannert Institute of Cardiology and the Division of Cardiology (B.J., S.-F.L.), Department of Medicine, Indiana University School of Medicine, Indianapolis.
Correspondence to Igor R. Efimov, Department of Biomedical Engineering, Washington University, One Brookings Dr, St Louis, MO 63130; E-mail igor@wustl.edu or to Shien-Fong Lin, PhD, Krannert Institute of Cardiology and the Division of Cardiology, Department of Medicine, Indiana University School of Medicine, Indianapolis, IN; E-mail linsf@iupui.edu


*Circulation Research* **is available at http://circres.ahajournals.org** **DOI: 10.1161/CIRCRESAHA.109.209841**

| Non-standard Abbreviations and Acronyms | |
|---|---|
| **AP** | action potential |
| **AVN** | atrioventricular node |
| **CMOS** | complementary metal oxide semiconductor |
| **CT** | crista terminalis |
| **DD** | diastolic depolarization |
| **LCR** | local subsarcolemmal ryanodine receptor-mediated $Ca^{2+}$ release |
| **LDCAE** | late diastolic $Ca_i$ elevation |
| **OAP** | optical action potential |
| **RA** | right atrium |
| **SAN** | sinoatrial node |
| **SACT** | sinoatrial conduction time |
| **SR** | sarcoplasmic reticulum |
| **SSS** | sick sinus syndrome |

published a year earlier by Tawara.[2] Following these morphological discoveries, Lewis[3] and Wybauw[4] presented electrophysiological evidence that the SAN is the site of origin of heartbeat.

In the last decade, SAN studies have led to important advances in unraveling the basic electrophysiological and molecular mechanisms associated with primary pacemaker activity.[5,6] These studies have made great contributions in deciphering SAN structure and function, allowing for new and exciting therapeutic strategies, including the creation of artificial biological pacemakers for the treatment of SAN disease.[7] Despite the past century of landmark SAN studies, much is still to be learned.

Optical mapping with voltage-sensitive dyes is currently the best available technology to investigate SAN structure and function because it allows the recording of simultaneous changes in the activation pattern and action potential (AP) morphology from multiple sites.[8] Optical signals represent a weighted average of transmembrane recordings collected from a volume of tissue with a space constant of several millimeters,[9–11] making the interpretation of what is happening within the tissue in its entirety extremely challenging. Recently 2 groups applied high resolution optical mapping techniques to investigate the canine SAN and found differing results because of different interpretations of optical mapping data.[12,13] This review and subsequent correspondence describes the anatomic structure of the SAN and proposed hypotheses governing impulse generation based on the available literature.

## Anatomy and Function of the Sinoatrial Node: Evolution of Methodology

The SAN is anatomically located at the junction of the superior vena cava and right atrium (RA) in the mammalian heart.[1,14,15] The SAN of the normal adult human heart is a relatively small intramural structure that is 10 to 20 mm long and 2 to 6 mm wide. It has an ellipsoid-like structure. The superior part (head) lies less than 1 mm beneath the epicardium, separated from that surface by a layer of connective tissue and fat. The SAN spreads from its head inferiorly for 10 to 20 millimeters remaining beneath the sulcus terminalis and just above the crista terminalis.[14–17]

The first detailed investigation of the dynamic change of the site of origin of excitation was done by Meek and Eyster in 1913 to 1914.[18,19] They found that the slowing of the heart rate through vagal stimulation or by cooling correlates with the migration of the site of the pacemaker from its original location within the SAN to either inferiorly within the SAN or to the AV node. These studies became the foundation for the hypothesis of the existence of a distributed pacemaker complex.

The next important step in the investigation of the SAN was made after the development of microelectrode techniques allowing the direct measurements of transmembrane AP arising from specialized pacemaker s tissue by Trautwein and Zink in 1952.[20] Following their work, de Carvalho et al[21] investigated the site of origin and pattern of excitation in the rabbit atrium by using intracellular glass microelectrodes. In 1965, Sano and Yamagishi[22] performed the first systematic mapping of the rabbit SAN region using 2 microelectrodes. They observed highly anisotropic spread of activation from the SAN: starting in the leading pacemaker, the AP propagated preferentially in an oblique cranial direction toward the crista terminalis (CT) and appeared to block in the direction of the septum, an observation confirmed later by many groups.[23–25] They and then Bleeker et al[26] calculated the conduction velocity near the leading pacemaker site to be 2 to 8 cm/sec or less.

Recently, we investigated activation patterns in the rabbit SAN using optical mapping,[27] which is the only available technology that allows the resolution of simultaneous changes in the activation pattern and AP morphology from multiple sites. Our activation maps of rabbit SAN region agree with maps obtained earlier using electrode-based mapping techniques.[26,28] In this study, we also demonstrated that the rabbit SAN is functionally and anatomically insulated from the atrial septum.[27]

However, the rabbit SAN is essentially a 2D structure.[26] This makes it easier to study but raises concerns of its relevance to the 3D structure of the canine[29–31] or human[14,32] SAN. Although the origin of SAN primary pacemaker activity has been extensively studied in many small animal species, it is virtually unexplored in man.[33] The functional studies of the human SAN function are complicated by the inability of epi- or endocardial mapping to detect the origin and slow propagation of AP within the intramural SAN layers before it activates the adjacent atrial myocardium.[12,29,34] Epicardial[32,35] and endocardial[36] mapping studies demonstrated widespread sites of the earliest atrial activation, as well as multifocal activation (activation started in 2 to 5 points located $>1$ cm apart) during normal sinus rhythm in humans. The atrial breakthroughs could arise at the epicardium and/or endocardium from a region along the crista terminalis (up to 7.5 cm[32,36] in length) that is significantly larger than the area of the anatomic SAN (which is only $\approx 1$ to 2 cm[14,16]).

Several hypotheses were proposed to explain these unclear relations between anatomy and function of SAN.[34] One of

them, the Boineau–Schuessler SAN model,[34,37] hypothesized discrete sinoatrial exit pathways, to explain how the atrial surface activation can be initiated from multiple sites simultaneously, as well as to describe the complex conduction within the SAN, which was inferred from a limited number of intracellular microelectrode recordings. The cardiac impulse arising from the SAN slowly propagates through the SAN and transmits to the atria via the several specialized conduction exit pathways (sinoatrial exit pathways). Recently, we confirmed this hypothesis for the canine SAN, which is very close both structurally and functionally to the human SAN.[29,31] We have extended high-resolution optical mapping to obtain optical AP (OAP) recordings from multilayer tissues and developed an analytic signal processing approach to resolve the intramural activation pattern of the canine SAN from the activation in the intervening epicardial and endocardial layers.[12] Thus, we directly demonstrated that the canine[12] and human[38] SAN is functionally insulated from the surrounding atrial myocardium except for several sinoatrial exit pathways.

Any experimental result is only as good as the methodology and data interpretation behind it. Our optical signal analysis is based on the following considerations described below.

## Physical Principles of Optical Recordings From Complex Multilayer Tissues Such As Sinoatrial and Atrioventricular Nodes

Physical principles of biophotonic imaging are based on several modalities of light scattering in biological tissues. It was shown in numerous studies using different biophotonic modalities that the depth penetration of optical probes in muscle tissues varies from several hundred micrometers to several millimeters.[39] The principles of fluorescence and light scattering underlie optical mapping with voltage- or calcium-sensitive dyes in the heart. It has been shown that signals recorded from cardiac tissue stained with these dyes carry information from 0.5 to 3 mm, depending on the excitation and emission spectra of corresponding molecular probes, as well as the scattering properties of the tissue.[9–11,40–42]

Light scatters in dyed tissue through 3 processes: scattering of excitation light propagating through tissue, fluorescent scattering at the fluorophore, and scattering of emission light propagating toward optical detector (Figure 1A). As a result of this complex process, the final optical signal is essentially a weighted average of electric activity arising from multiple layers of cells within the tissue to a depth governed by a space constant, which is determined by light scattering and absorption properties. As shown in Figure 1B, the space constant for both excitation and emission of light in cardiac tissue is 1.5 to 2.0 mm, which corresponds to the entire thickness of the canine SAN or rabbit atrioventricular node (AVN).

Figure 1A shows optically recorded signals collected from different regions of a canine SAN, published in our recent study.[12] When an AP is optically recorded by a photodiode arising only from the atrial myocardium or only from the SAN, it corresponds well with the well-known single-cell responses from the atrial and SAN myocytes (Figure 1A, top left). However, when an optical signal is recorded over a sandwich of atrial and SAN tissues, the resulting signal is a summation of APs. During physiological activation, the SAN AP always precedes atrial activity because of sinoatrial conduction delay. The resulting signal has 2 distinct components, as shown on the top right of Figure 1A. Interestingly, because of the slight elevation in the anatomic position[31,12] of the SAN within the right atrial wall, SAN tissue almost reaches the endocardium near its inferior end and emerges at the epicardium on the superior end. As a result, the optical signals recorded from the inferior to superior endocardial projection of SAN (Figure 1A, bottom) have progressively smaller and smaller SAN components and larger atrial components. Similarly, epicardial recordings will have a reversed relationship between SAN and atrial components along the superior-inferior axis (not shown).

If these physical principles are not enough to convince the reader that multiple components of the OAP arising from SAN exist because of multiple layers of tissue being imaged, we offer a direct physiological validation.

## Physiological Validation of the Multiple Components in the Rabbit AVN and Canine SAN

Our study of the rabbit AV node[40] has clearly demonstrated that using simultaneous recordings with microelectrode and optical mapping of this 0.5 to 1.0 mm thick structure yields a biphasic optical signal. During anterograde conduction, the first component carries the signature of the superficial layer of atrial myocardium and the second component documents excitation of the AV node and the bundle of His (Figure 2A and 2B). When we paced at the His bundle and induced retrograde conduction, the sequence of the 2 components was reversed: His-AVN excitation was observed in the first component, whereas the atrial layer was documented in the second component.[43] Thus, such complex biphasic optical signal cannot be interpreted as a response of a singe cell. Complex multiphasic optical recordings often represent asynchronous excitation of different groups of cells or cell layers from within the path of light, that the optical detector collects. Familiar OAPs resembling microelectrode recordings arise only in the cases of well-coupled syncytium, such as uniform working ventricular myocardium. Canine and human SAN and AVN are not such well-coupled uniformed structures (Figures 1A, 2C, and 2D). Figure 2C and 2D shows transient SAN exit block following 10 minutes of pacing. OAP tracings demonstrate slow, small amplitude signals, which reflect only the SAN APs without an atrial component, because the atria were not excited by SAN. This SAN wave originated near the same site observed before pacing but was blocked superiorly and slowly propagated to the inferior aspect of the SAN. However, the next SAN activation successfully exited from both exit pathways and simultaneously excited atrium. These observations were consistent in all SAN preparations (n=4) in which SAN exit block was observed.[12]

Thus, optical signals recorded from the SAN of a large mammal will typically yield multiphasic optical recordings representing asynchronous excitation in different layers of tissue. Normally the SAN fires first and then after a 35 to 95ms delay[34,37] the atrium fires. Thus, the optical signals will

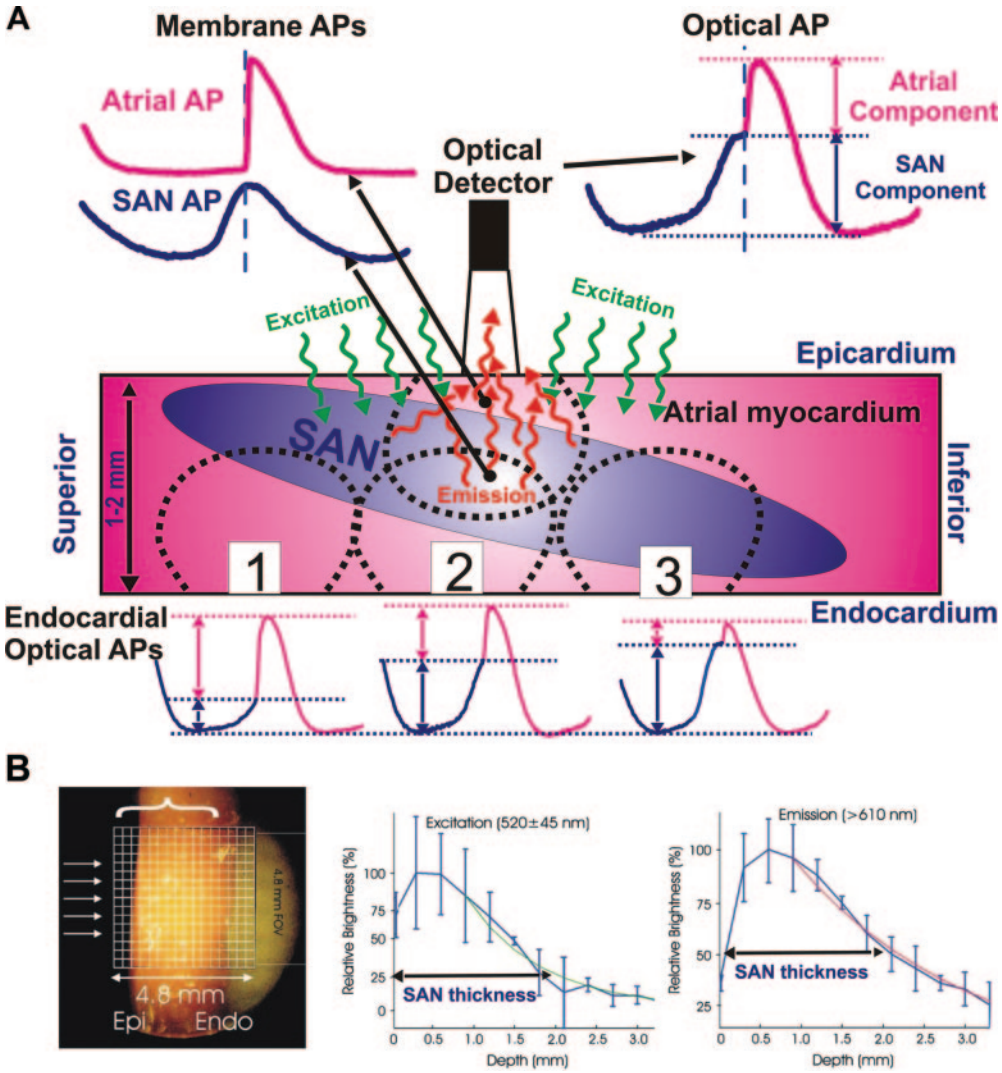


**Figure 1.** Mechanism of the double components of the OAP recording from canine SAN tissue. A, Simplified model of the SAN based on published data.[12] This "section" cuts along the superior-inferior axis of SAN. Top Left, OAP recordings[12] from only atrial and only SAN layers of tissue, which closely resemble morphology of microelectrode AP recordings. Top Right, OAP[12] recording from an area encompassing both atrial and SAN tissue layers, thus averaging APs from both structures. Bottom, OAPs from different SAN regions.[12] B, Depth penetration measurements for excitation wavelength. Modified from Bishop et al[11] with permission.

contain 2 components representing a weighted average of these 2 electric activities: a relatively small signal from the deeper SAN layer and more robust signal from the atrial layer of epicardium or endocardium. In our interpretation, we followed this logic and thus disagree that one of the optical components can be interpreted as trigger activity (delayed afterdepolarization or early afterdepolarization) without further validation from microelectrode recordings.

## Analysis of the Multiple Components of the Optical Recordings From SAN

Figure 3A shows the detailed analysis that was used to separate the SAN optical signal component from the atrial components in OAPs. The optical signals were filtered using the low-pass Butterworth filter at 200 Hz. Traditional criteria for measuring activation times ($AP_{50}$ and $dV/dt_{max}$) did not show activation of the SAN layer because of relatively small SAN optical components in most recording sites. Only by separating the 2 upstroke components was it possible to distinguish SAN activation (see Figure 3B). Separation of the components allowed for measurement of the maximum of the first derivative ($dV/dt_{max}$), OAP amplitude, and conduction velocity in individual tissue layers. We also found that the 50% of the OAP amplitude ($AP_{50}$) map more precisely reflected the SAN conduction than the $dV/dt_{max}$ map because of the weak dV/dt of the slow SAN upstroke. The AP amplitude of each component was measured as the difference between the minimum and maximum fluorescence in this component. In most cases, the amplitude of the SAN component of the OAP was less than the atrial component because of light attenuation and scattering during propagation from deeper structures (see Figures 1A and 3C). The optical signals from the block zone (intraatrial septum margin of the SAN) contains a double-component upstroke because of scattering and electrotonic effects of the 2 different atrial layers (see also figure 8C from the study by Bromberg et

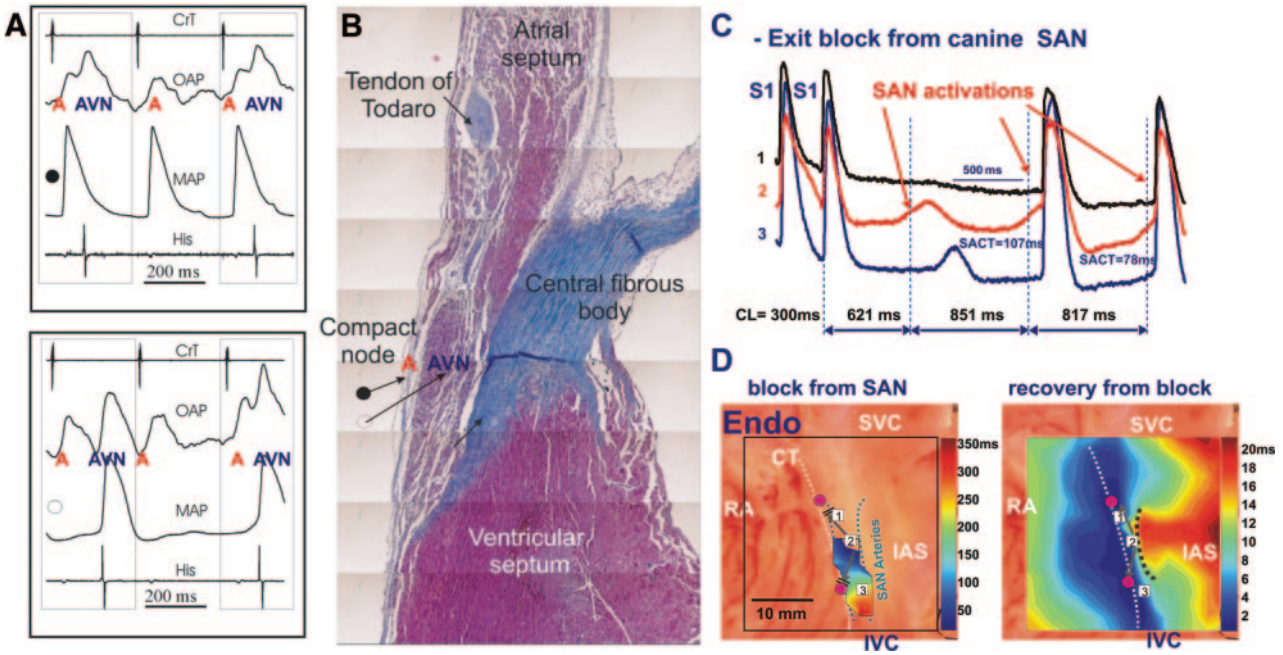


**Figure 2.** Physiological validation of the multiple components in the rabbit AVN and canine SAN. A, Simultaneous optical recordings from the distal AVN and bipolar electrograms from the atrial input to the AVN and from the bundle of His. A flouting glass microelectrode was used to impale cells in different AVN layers (black and white circles). Recording panels illustrate 3 consecutively paced beats during Wenchebach 2:1 block with simultaneously acquired atrial inputs and His electrograms, along with optical and microelectrode signals.[40] B, Histology shows a section of the rabbit heart through approximately the same area, which was functionally documented in A. C and D, OAPs during transient SAN exit block demonstrate separation of 2 components: SAN and atrial. Modified from Figure 6 of Fedorov et al.[12] IAS indicates intraatrial septum; IVC, indicates inferior vena cava; SVC, superior vena cava; RAA, right atrial appendage.

al[29]). The slope of the slow diastolic depolarization was determined by measuring the slope of a linear fit of depolarization and normalizing it to the OAP amplitude (Figure 3A). Slow diastolic depolarization phase was clearly distinguishable from upstroke of the SAN potential (first OAP component).

### Simultaneous Voltage and Calcium Recordings From the Canine SAN

Recently, we conducted 3 canine optical mapping SAN experiments simultaneously using both voltage-sensitive dye RH237 and calcium-sensitive dye Rhod-2 AM (V.V.F., A. V. Glukhov, R. B. Schuessler, V. G. Fast, I.R.E., unpublished data, 2008). A halogen lamp (250 W) was used for the excitation light, which we filtered with a 520±45-nm band-pass filter. Emitted light was filtered by 700-nm long-pass filter for voltage signal, and filtered with a 585±10-nm band-pass filter for the calcium ($Ca^{2+}$) signal. Fluorescent signals were recorded from the epicardial optical field of view (30×30 $mm^2$) with a spatial resolution of 300 $\mu$m/pixel at a rate of 1000 frames/s using two 100×100 Ultima-L complementary metal oxide semiconductor (CMOS) cameras (SciMedia, Japan). The optical signals were filtered using the low-pass Butterworth filter at 32 to 100 Hz. We found in all 3 experiments that both the voltage and calcium optical signals from SAN region contain 2 upstrokes during normal sinus rhythm. Figure 4 shows an example of dual voltage and $Ca^{2+}$ optical mapping of the canine SAN. Both the upstroke components of voltage optical traces always precedes calcium upstrokes by 7 to 20 ms. We also found, as shown previously in Figure 2C and 2D, that atrial pacing depressed SAN conduction and in turn caused the separation of the SAN and atrial components (Figure 4D). Figure 4D clearly shows SAN signals with the beginning of the repolarization phase for both voltage and calcium recordings. The voltage double upstroke area of the SAN (blue dotted oval) coincided well with the $Ca^{2+}$-detected double-upstroke area (green dotted line ellipsoid) (Figure 4C). Moreover, we found that 10-minute perfusion with ryanodine (5 $\mu$mol/L) decreased calcium signals more than 5-fold but did not significantly change SAN cycle length (550 to 559 ms) nor the double-upstroke components of the voltage optical signals from the SAN. Thus, we demonstrated that the first component of the SAN OAPs is the upstroke of pacemaker APs, whereas the second component belongs to the atrium.

The highest spatial resolution of our optical photodiode mapping system (photodiode array) was 562×562 $\mu m^2$ per photodiode (Figure 3). Our MiCAM ULTIMA system has higher resolution than photodiode array (up to 300×300 $\mu m^2$ per pixel) and yields similar signal morphologies (Figure 4). However, the CMOS pixel resolution is below the point spread function in tissue, and therefore the actual optical resolution, limited by the point spread function, is in this preparation ≈500 to 1000 $\mu$m.[44]

## Part II. By Boyoung Joung and Shien-Fong Lin

Although it has been shown more than 40 years ago that spontaneous diastolic depolarization of SAN cells initiates

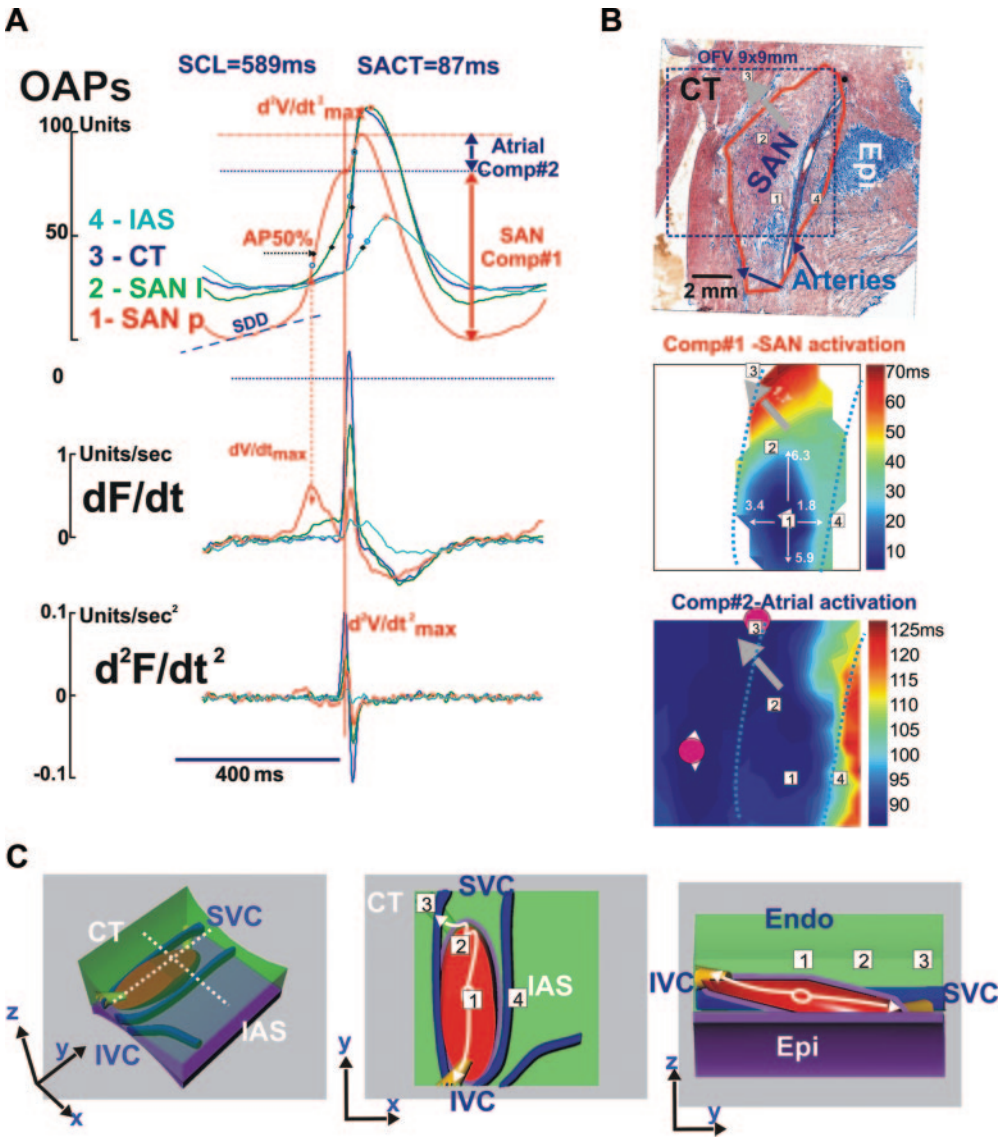


**Figure 3.** Analysis of optical transmembrane potentials from canine the SAN. A, OAPs and their first (dV/dt) and second ($d^2V/dt^2$) derivatives during normal sinus rhythm from photodiodes recordings shown in B. OAPs were separated into the SAN and atrial components using the $d^2V/dt^2$max of the signal as the transition point. B, Parallel histology section to the epicardial (Epi) surface with 9×9 mm optical field of view (blue dotted square) is shown by a dark blue dotted rectangle. Activations maps of the SAN and atrial components of the OAPs (modified from figures 2 and 5 of the study by Fedorov et al[12]). C, Three-dimensional model of SAN, a 3D model of the canine SAN (modified from figure 8 of the study by Fedorov et al[12]).

APs to pace the heart,[45] the mechanism of heart rhythm generation is still controversial. The spontaneous diastolic depolarization has traditionally been attributed to a "membrane clock" mechanism, mediated by voltage-sensitive membrane currents, such as the hyperpolarization-activated pacemaker current ($I_f$).[46,47] Recently, it has been extensively demonstrated that the spontaneous rhythmic local $Ca^{2+}$ release events from sarcoplasmic reticulum (SR) of SAN, manifested as $Ca^{2+}$ sparks, work as a "$Ca^{2+}$ clock," causing diastolic depolarization via activation of $I_{NCX}$, which coordinately regulates sinus rate along with the membrane clock.[48–59] Thus, a more complete picture of pacemaking at the cellular level emerges from these studies. It remains to be established how the cellular pacemaking mechanisms can be applied to SAN function at the tissue or organ level.

The cardiac automaticity at the organ level is a very complex phenomenon and, besides cellular mechanisms, other integrative factors are also involved. The intact SAN is a heterogeneous structure that includes multiple cell types interacting with each other,[60–63] the relative importance of the voltage and $Ca^{2+}$ clocks for pacemaking in different regions of the SAN, and in response to neurohumoral stimuli such as $\beta$-agonists, may be different. Indeed, activation maps in intact canine RA showed that SAN impulse origin is multicentric,[64] and sympathetic stimulation predictably results in a cranial (superior) shift of the pacemaking site in human and dogs.[37,65] Moreover, the response to drug or genetic mutation is different between single cell and intact SAN. These findings suggest that after the leading pacemaker cell fails to work properly, other cells generate the rhythm in intact tissue. Previous evidence from

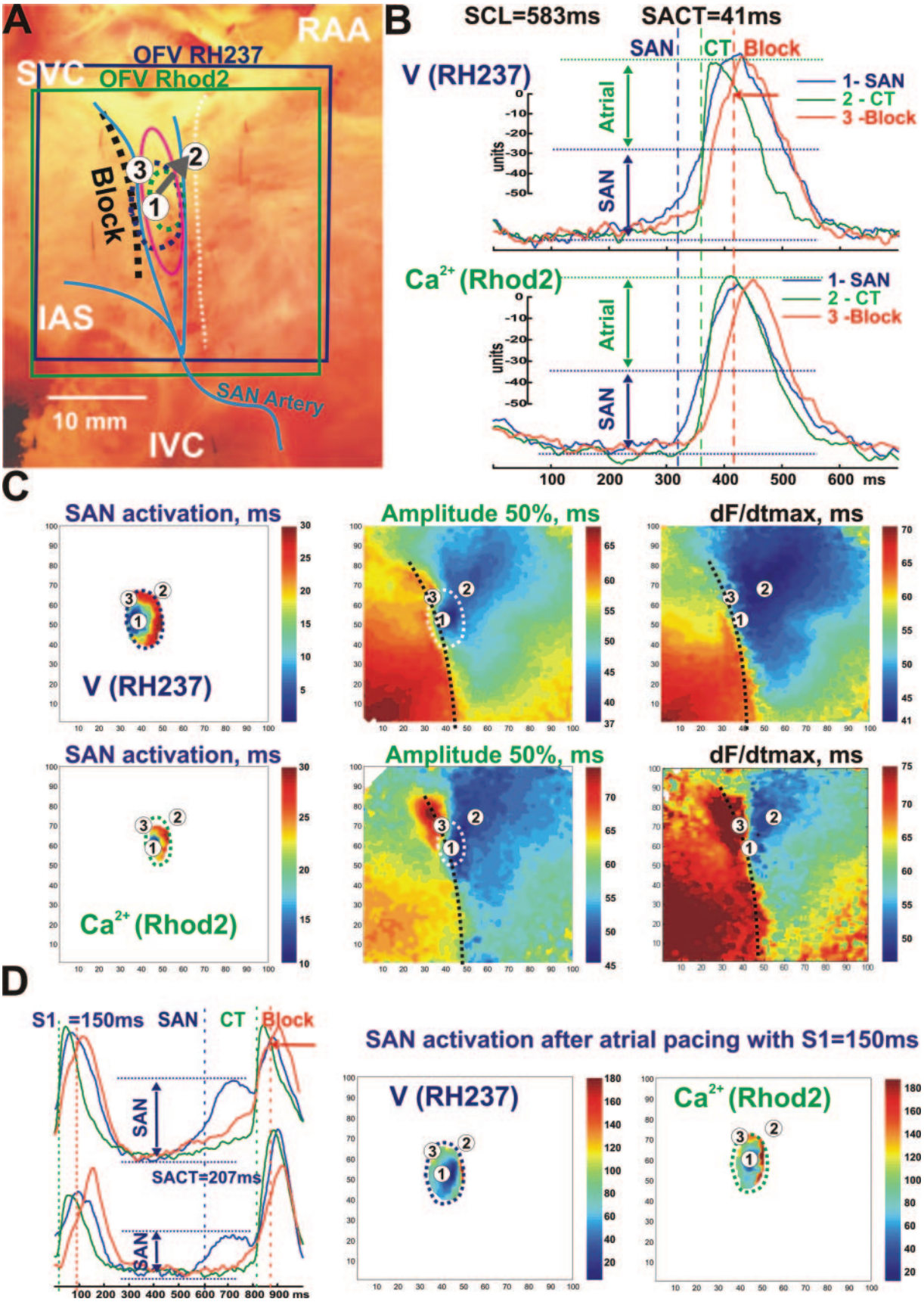


**Figure 4.** Simultaneous voltage and calcium epicardial optical mapping of the canine SAN. A, Epicardial photographs of a perfused canine atrial preparation with 2 optical field of views for voltage sensitive dye RH237 and $Ca^{2+}$ sensitive dye RHOD2. The SAN arteries are shown by blue curves. The red oval shows the approximate border of the SAN region. IAS indicates intraatrial septum;

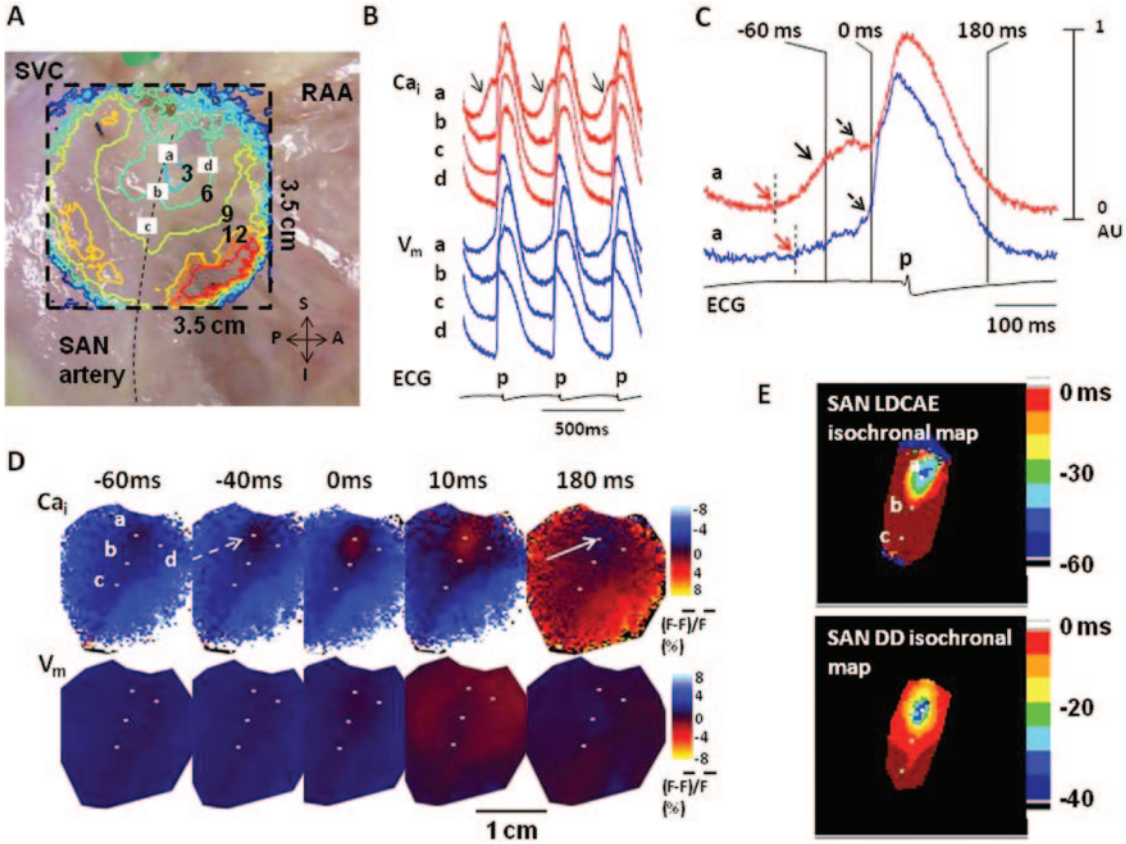


**Figure 5.** Activation pattern of SAN and surrounding RA during 0.3 $\mu$mol/L isoproterenol infusion. A, Isochronal map of $V_m$. The number on the each isochronal line indicates time (ms). B, The $V_m$ (blue) and $Ca_i$ (red) recordings from the superior (a), middle (b), and inferior (c) SANs and the RA (d) are presented. C, Magnified view of $Ca_i$ and $V_m$ tracings of the superior SAN. Note the robust LDCAE (solid arrow) before phase 0 of the AP (0 ms), which in turn was much earlier than the onset of the p wave on ECG. D, The $V_m$ and $Ca_i$ maps from −60 ms before to 180 ms after phase 0 of the AP of C. The LDCAE (broken arrows in frames −40 and −20 ms) was followed by the $Ca_i$ sinkhole during early diastole (solid arrow in frame 180 ms). E, The SAN LDCAE (top) and DD (bottom) isochronal maps. Note the colocalization of the LDACE and DD. Modified from Joung et al.[13]

isolated SAN myocytes showed that late diastolic $Ca_i$ elevation (LDCAE) relative to the AP upstroke is a key signature of pacemaking by the $Ca^{2+}$ clock. This criterion could provide insights into the relative importance of the $Ca^{2+}$ and voltage clock mechanisms of pacemaking in intact SAN tissue.[13]

## The $Ca_i$ Dynamics in Intact Canine SAN

In contrast to the single SAN cell confocal $Ca_i$ imaging,[55–59] the spontaneous diastolic SR $Ca^{2+}$ release manifested by the LDCAE was observed in only a small percentage of the baseline preparations. However, the LDCAE occurred in all preparations during isoproterenol infusion and was associated with a superior shift of the leading pacemaker site coincident with the appearance of robust LDCAEs (Figure 5) in this region. Most importantly, the site of maximum LDCAE slope always colocalized with the leading pacemaking site, suggesting a paradigm shift in which the voltage clock now lagged behind the $Ca^{2+}$ clock (Figure 6). With $\beta$-stimulation, the dominant pacemaking site gradually shifted in the SAN from inferior to superior with the increase of heart rate and dosage of isoproterenol (Figure 6A). Colocalization of LDCAE and the dominant SAN activation site became obvious as the heart rate increased. Slopes of LDCAE and diastolic depolarization (DD) both increased with heart rate (Figure 6B).

The $Ca_i$ dynamics of SAN was characterized not only by the earliest onset of LDCAE, but also by the fastest $Ca_i$ reuptake as compared with other RA sites. The baseline 90% $Ca_i$ relaxation time was shorter at the superior SAN than at other RA sites. This resulted in the formation of the $Ca_i$ sinkhole, which was facilitated by a rapid decline (short relaxation time) of the $Ca_i$ fluorescence at the superior SAN during isoproterenol infusion and suggests that $Ca_i$ reuptake by the SR is fastest in the superior SAN. The key protein regulator of SR $Ca^{2+}$ uptake is phospholamban, which inhibits SERCA2a in the dephosphorylated state. There was a significantly lower SERCA2a/phospholamban ratio at SAN sites than at RA sites, suggesting more phospholamban molecules are available to regulate SERCA2a molecules in

**Figure 4. (Continued).** IVC, indicates inferior vena cava; SVC, superior vena cava; RAA, right atrial appendage. B, OAPs and intercellular $Ca^{2+}$ traces from the center of the SAN (1), the atrial breakthrough in CT (2), and block area (3) from sites 1 to 3 in A and C during normal SR. C, Separated SAN and atrial activation maps ($AP_{50}$ and $dV/dt_{max}$) obtained by both dyes. D, OAPs and intercellular $Ca^{2+}$ traces; 3 recording sites shown in the activation maps (right) following the termination of atrial pacing with an S1S1=150 ms and recovery of spontaneous SAN activity (V.V.F., A. V. Glukhov, R. B. Schuessler, V. G. Fast, I.R.E., unpublished data, 2008).

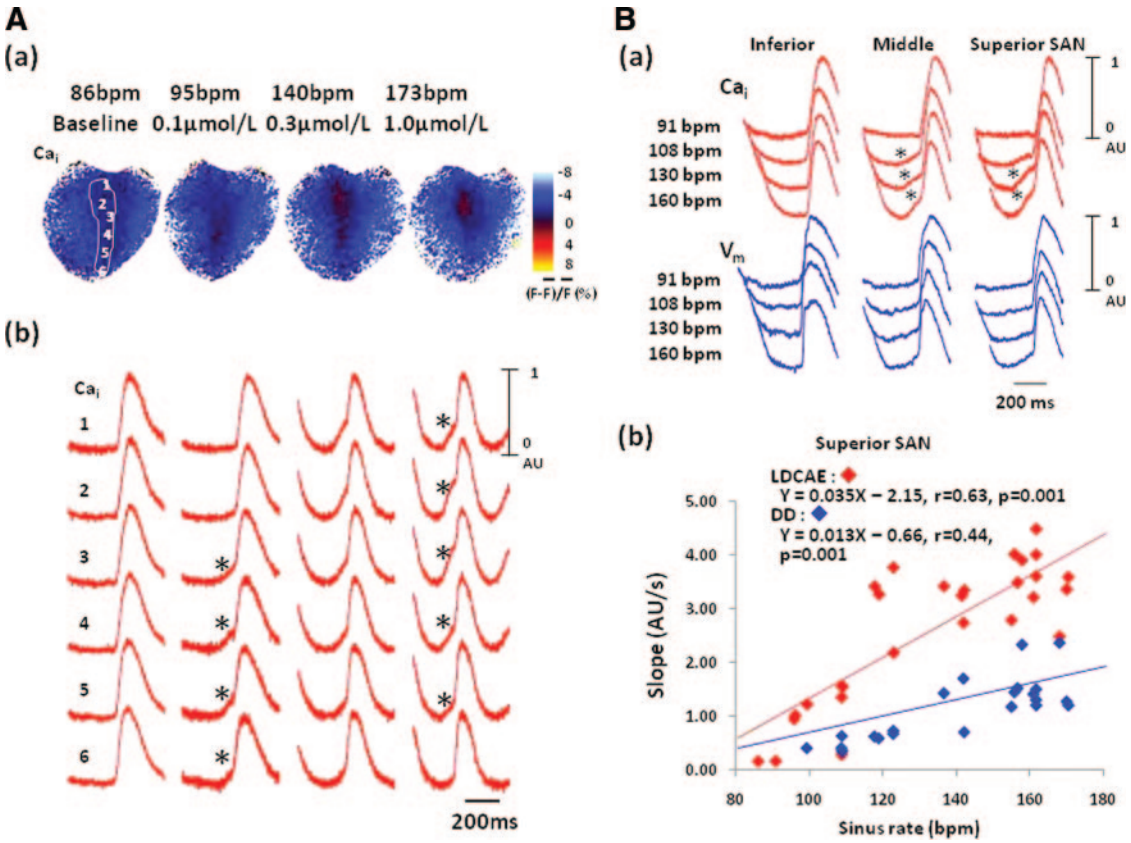


**Figure 6.** Colocalization of LDCAE and the leading pacemaking site. A, Upward shift of the leading pacemaking site with LDCAE during isoproterenol infusion. a, $Ca_i$ ratio maps of SAN at the respective sinus rate. b, Corresponding $Ca_i$ tracings from the superior,[1,2] middle,[3,4] and inferior[5,6] SAN. At 95 bpm, sites 4 and 5 had the most prominent LDCAEs (asterisks). As the sinus rate gradually increased, the sites of $Ca_i$ elevation progressively moved upward. At the maximum sinus rate of 173 bpm, site 2 had the most apparent LDCAE. B, Differential responses of different SAN sites to isoproterenol. a, The $Ca_i$ and $V_m$ tracings from the inferior, middle, and superior SAN sites at different sinus rates. b, The LDCAE and DD slopes of the superior SAN at different sinus rates. Reproduced from Joung et al[13] with permission.

SAN than in RA. Isoproterenol infusion phosphorylates phospholamban and relieves phospholamban inhibition of SERCA2a, which may account for more robust $Ca^{2+}$ uptake in SAN than in RA during isoproterenol infusion.[13]

## Evaluation of SAN Function by Pharmacological Interventions

The SAN $Ca_i$ dynamics responded to various interventions. The rate of LDCAE was increased by isoproterenol infusion and caffeine injection with the increase of heart rate. Blocking the SR $Ca^{2+}$ release consistently abolished LDCAE and decreased heart rate. In single SAN cells, ryanodine suppressed heart rate by 52% and 95% at the dosage of 3 and 30 $\mu$mol/L, respectively.[55] However, the ryanodine-induced heart rate decrease (20% at the 30 $\mu$mol/L)[13,66] was much less in intact SAN than in single SAN cell. This discrepancy can be explained by the compensatory rhythm generation from other parts of the SAN tissue, and by the activation of subsidiary pacemakers in the RA. In addition, such difference between spontaneous activities of isolated SAN cells and the intact SAN/ heart may be accounted for by a heterogeneous distribution of cyclic nucleotides or network properties of the intact tissue. In intact RA, a cell or a small group of cells at certain region of SAN may function as the "leading" pacemaker at a given time point. In case this leading pacemaker stops generating APs, another region of SAN may take over and generate sinus rhythm. Only if there is a considerable amount of 'silent' cells present at the same time, SAN pacemaking is interrupted. When this occurs, an ectopic pacemaker may take over and activate the RA. Complete suppression of all pacemakers is needed to prevent heart rhythm generation.

Previous results of the effect of $I_f$ blocker on heart rate have been variable. In isolated rabbit RA preparations, $Cs^+$ (2 mmol/L), UL-FS-49 (1 $\mu$mol/L), and ZD-7288 (3 $\mu$mol/L) decreased the spontaneous rate by 12%, 16%, and 13%, respectively.[67] However, Leitch et al reported that ZD 7288 of 0.64 $\mu$mol/L reduced heart rate at −53% and −38% in guinea pig SAN and rabbit heart, respectively.[68] In freely beating nonpatched cells, 2 mmol/L CsCl caused a 30% reduction in rate of beating.[69] However, even with $I_f$ blockade, isoproterenol still increased LDCAE and heart rate in our study.[13] As presented in previous experiments,[13,66] blocking either $Ca^{2+}$ clock or membrane clock did not produce sinus arrest, but sinus arrest was easily induced by the simultaneously blocking of both clocks.[70] This finding supports the idea that these 2 mechanisms of automaticity work synergistically to generate sinus rhythm. This redundant system

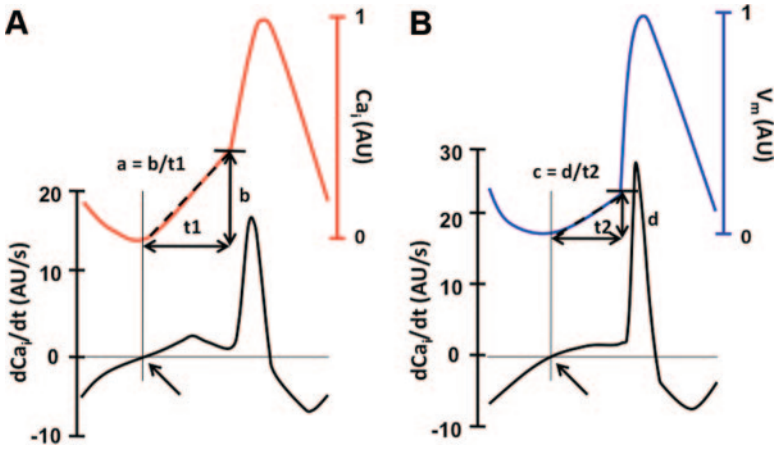


**Figure 7.** Schematic explanation of how the slope of LDCAE (A) and DD (B) were measured. The slopes of LDCAE and DD were measured from the onsets of LDCAE and DD to peak levels of LDCAE and DD, respectively. The onsets of LDCAE and DD were defined by the time of the transition between negative to positive values in $dCa_i/dt$ and $dV_m/dt$ curves (arrows).

ensures heart rhythm generation when one of the mechanisms is compromised.

## Evaluation of SAN $Ca_i$ Dynamics in Diseased Hearts

Sick sinus syndrome (SSS) is an abnormality involving the generation of the AP by the SAN and is characterized by an atrial rate inappropriate for physiological requirements. SSS is a collection of conditions with multiple causes.[71] The remodeling of SAN by aging[72,73] or diseases such as heart failure[74,75] and atrial fibrillation[76,77] are reported as the cause of the SSS. In familial SSS, the mutations of $Na_v1.5$,[78,79] HCN4,[80] ankyrin-B,[81] and ryanodine receptor[82] were found as the causes of SSS. Our laboratory has reported the existence of prolonged sinus pause in a canine model of pacing-induced heart failure.[83] However, whether the impairment of "membrane clock" and/or "$Ca^{2+}$ clock" mechanisms can produce SSS model is still unclear.[6,66,84]

SAN dysfunction is frequently associated with atrial tachyarrhythmias. Abnormalities in SAN pacemaker function after termination of tachycardia can cause syncope and require pacemaker implantation, but underlying mechanisms remain poorly understood. Recently, Yeh et al[85] reported that atrial tachyarrhythmias downregulate SAN HCN2/4 and minK subunit expression, along with the corresponding currents $I_f$ and $I_{Ks}$. Tachycardia-induced remodeling of SAN ion channel expression, particularly for the "pacemaker" subunit $I_f$, may contribute to the clinically significant association between SAN dysfunction and supraventricular tachyarrhythmias. Interestingly, downregulation of $I_{CaL}$ was not observed in this model, and this study did not evaluate the $Ca^{2+}$ clock function. Incidentally, downregulation of HCN4 and HCN2 expression has also been contributed to heart failure-induced sinus node dysfunction.[86] We studied a pacing-induced atrial fibrillation canine model with SAN dysfunction. The isoproterenol-induced heart rate acceleration and LDCAE in superior SAN were severely impaired.[87] Also the type 2 ryanodine receptor in the superior SAN of AF dogs in this model was downregulated to 33% of normal. Taken together, these findings suggest the impairment of both membrane and $Ca^{2+}$ clocks is responsible for SAN dysfunction caused by atrial tachyarrhythmia. SAN automaticity is significantly impaired only when both "clocks" fail to operate. Under such a condition, ectopic beats could emerge from subsidiary pacemaking sites.

Because of the intricate interaction of the membrane and calcium clocks[88] and the complicated tissue structure around the SAN, study of SAN function at tissue level in diseased conditions will remain a significant challenge. Future works along this line of study require close collaboration between the mathematical modelers and experimenters to dissect the role of individual components. Furthermore, mathematical models of SAN function at the tissue level are urgently needed for this purpose.

## Analysis of Optical Mapping Data

The electrophysiological definition of SAN is very complicated. For electrophysiological location of the dominant pacemaker, several criteria have been mentioned in the literature: (1) earliest activation[22,29,89,90]; (2) fast diastolic depolarization[89,90]; (3) slow phase 0 depolarization[91,92]; and (4) gradual transition from diastolic into systolic depolarization.[90] According to the comparison of these criteria by Bleeker et al,[26] the configuration of the AP as the only criterion does not identify the dominant pacemaker site. In our study,[13] the SAN region was defined by the imaging areas showing the earliest activation and fast diastolic depolarization in normal conditions.

The $Ca_i$ and $V_m$ traces were normalized to their respective peak-to-peak amplitude for comparison of timing and morphology. The slopes of LDCAE and DD were measured from the onsets of LDCAE and DD to peak levels of LDCAE and DD, respectively. The onsets of LDCAE and DD were defined by the time of the transition between negative to positive values in $dCa_i/dt$ and $dV_m/dt$ curves (Figure 7). The "90% $Ca_i$ relaxation time" was measured from the maximum systolic $Ca_i$ to 90% reduction of $Ca_i$. RA $V_m$ isochronal map was generated by the traditional criteria for detecting activation times (50% of the OAP amplitude). The SAN DD and LDCAE isochronal maps as shown in Figure 5E were generated by the 50% of diastolic depolarization and $Ca_i$ amplitude before phase 0, respectively.

## Beauty Behind the 1-mm Curtain: Endocardial Mapping of Canine SAN

Fedorov et al demonstrated a double-component morphology in optical potentials of canine SAN using primarily an

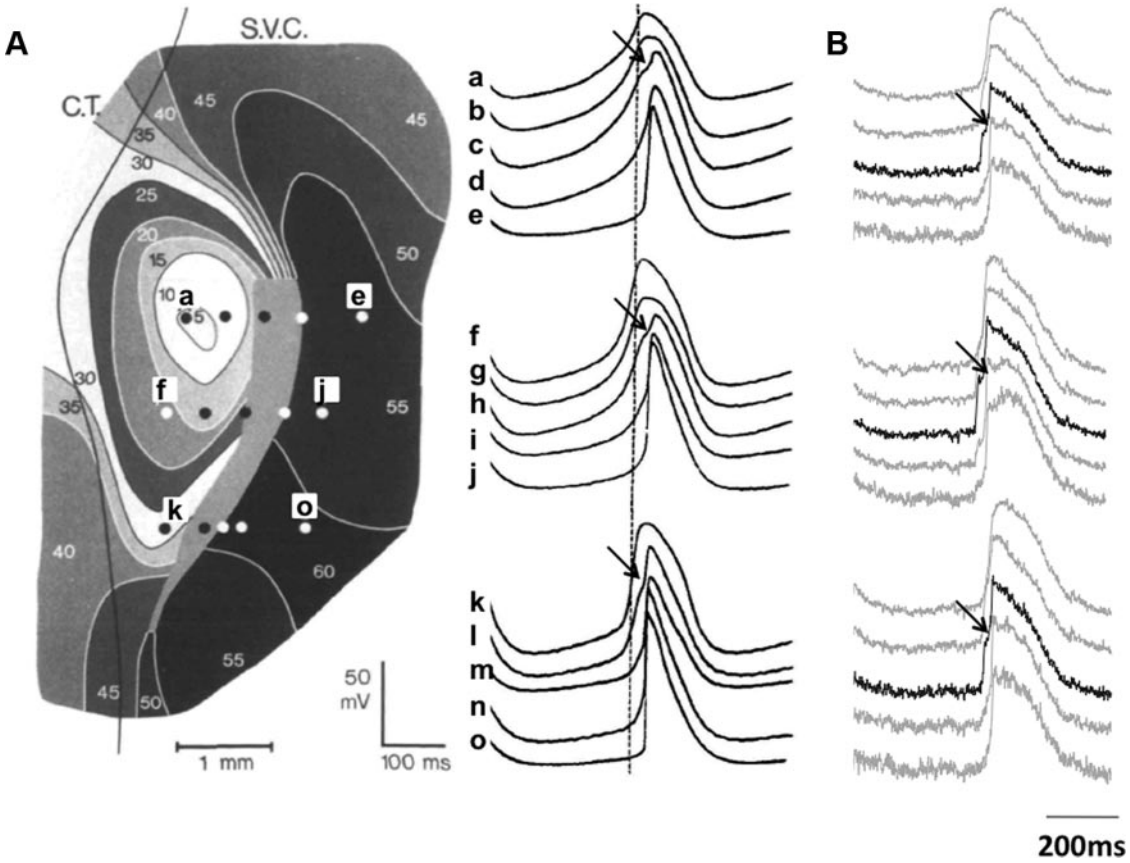


**Figure 8.** Identification of conduction block with double potentials in the sinus node. A, The APs (on the right side) were recorded at corresponding points of the activation map (on the left side). The dashed line indicates the time reference. The area in which double potentials (arrows) in the AP were clearly visible is hatched in the activation map (modified from Bleeker et al[26]). B, The $V_m$ tracings showing the double potentials (arrows) at the border of SAN.

endocardial mapping setup.[12] In fact, their results were derived almost entirely from the analysis of this double-component feature in the recording. Incidentally, epicardial mapping was also performed, but the results were not shown. On the other hand, the distinctive double-component OAPs were not observed in any of our 26 preparations, and all mapping studies were performed from the epicardial side. The SANs in humans[71,93] and in dogs[94] are both located beneath the epicardial surface at the upper portion of the crista terminalis. This anatomic aspect was also demonstrated in figure 7 of the study by Fedorov et al.[12] SAN is covered by only 0.2- to 0.4-mm fibrous membrane from the epicardial side. For this reason, the microelectrode recording can be readily performed from the epicardial side in dog hearts.[29,94] However, atrial muscle (> 1 mm) is present between the SAN and the endocardium. Consequently endocardial optically mapping of SAN through a layer of atrial myocardium can be significantly distorted and contaminated. Furthermore, SAN arteries of human and dog can be dilated by up to 1 mm at the mean aortic pressure,[93] and the arterial dilation that heterogeneously moves the SAN away from the endocardium could further distort the recording and affect the outcome of depth-resolved data interpretation.

The morphology of double potentials is not restricted to overlapping electric propagation in multiple tissue layers. Double potentials can be observed even in single cell recording when the cell is located at the boundary of discontinuous conduction.[26,95] Specifically, Bleeker et al[26] used such a double potential feature to identify the conduction block zone around the rabbit SAN (Figure 8A). The first component of these APs closely followed the AP of the pacemaker whereas the second component was nearly synchronous with activation at the edge of SAN. These double-component APs can be observed over an area with width of 0.2 mm to >1 mm. In fact, the most obvious double-component optical potentials in our data existed at the block zone (Figure 8B, middle dark traces). Figure 8 shows a comparison of the original intracellular recordings in the article by Bleeker and our optical traces at similar recording site. The complicated anatomic construct of SAN offers ample opportunities for discontinuous conduction and hence double-component optical potentials. It may be difficult to clearly identify the electrotonic or multiple-layer origin of the double components, but using double potential exclusively to derive conduction pattern from "two overlapping tissue layers" is obviously insufficient.

The spatial resolution of the imaging devices and optical configuration are additional considerations. Large pixel size allows more signals from the surrounding atrial tissue to be included in the fluorescence registered in that pixel and consequently helps to increase the signal-to-noise ratio attributable to the inherent spatial averaging. In a recent study by

Bishop et al using Monte Carlo simulation, the authors concluded that the scattering volume in a uniformly illuminated tissue is ≈3 times larger in the surface recording plane than in depth.[96] All of these physical considerations lead to the conclusion that multiple activations on the "surface" are more likely to be registered than in "depth." Furthermore, the depth of field of optical systems is directly proportional to physical pixel size among many other factors.[97] Therefore, large pixels of the optical sensors such a photodiode array could enhance the capability to record intramural optical signals. We also think that it is inappropriate to use 500 to 1000 $\mu$m as a universal limit for optical resolution because optical mapping has been successfully applied to small cardiac tissue such as chick and mouse hearts.[98–101] Lower spatial sampling (16×16 with photodiode arrays) is likely to create spatial aliasing when the structure of interest has higher spatial frequency content, such as at the elongated edge of the SAN. The subsequent interpolation of the activation time is a major flaw of the opponents' approach. The interpolation conveniently and artificially removes pixelation of the images with a presumed conduction pattern, most likely linear conduction, which is inconsistent with the SAN conduction.

### The Debate: Is Double Potential the Signature of SAN in Optical Mapping?

This debate is on defining the SAN activation based on the morphology of optical traces. Because our $Ca_i$ recording during $\beta$-stimulation (top trace in Figure 5B) resembles the double potential pattern, it may be interpreted as coming from different structures of the tissue. The double components reported by Fedorov et al[12] were observed after phase 0 of the RA AP. In contrast, the $Ca_i$ elevation related to rhythm generation during $\beta$-stimulation is located at the superior SAN during late diastolic period before phase 0 activation of RA. The superior SAN is directly below the epicardium (Figure 3C) where we mapped. Therefore, effects of the double layer should not influence the evaluation of $Ca_i$ dynamics during late diastole. An important concern in applying dual optical mapping of $V_m$ and $Ca_i$ to a thin and slowly conducting tissue such as the intact SAN is whether the different dyes are imaging equivalent volumes of tissue, because the dyes have different tissue penetration and scattering properties.[8] However, this concern is somewhat mitigated by the same site that did not exhibit LDCAEs under basal condition developed LDCAE after isoproterenol infusion, despite identical imaging parameters.

It is also unresolved why the distinctive double potential reported by Fedorov and Efimov was not observed in our $V_m$ recording. Our search for the double potential was initially misled by the "standard" morphology as shown in Figures 1 and 3. In Figure 3A, a typical presentation of the double potential from the SAN is first a slow DD, followed by a low-amplitude upstroke reaching plateau (SAN), and ended with a higher-amplitude second upstroke (RA). Other than the obvious amplitude difference between the 2 upstrokes, a sufficient time lag between them is also required for their separation. We were unable to identify such a "typical" double-potential pattern in our recordings. However, if a slow depolarization followed by a faster upstroke (Figure 4B, trace 1) is also referred to as double potential, then we have to agree that our data indeed showed "double potential" in the SAN region. However, without the first component reaching the plateau, our opponents did not show how to distinguish the DD and SAN components from their unpublished data.

## Part III. Vadim Fedorov and Igor Efimov Rebuttal

We would like to emphasize that we do not have disagreement with Drs Joung and Lin about the ionic pacemaker mechanisms of the SAN. We agree that both the voltage and calcium clocks are very important in the maintenance of SAN pacemaker activity. Thus, most of our disagreement is related to the interpretation of optical mapping data, which we would like to address in our rebuttal.

1. The main difference between the 2 groups is that our group was able to record not only slow diastolic depolarization but also the pacemaker upstroke (first component of the OAPs upstrokes). Based on this upstroke, we can reconstruct canine SAN activation patterns during normal rhythm (Figure 3), which Joung et al[13] are unable to do given their methodology and subsequent findings. To recapitulate, we can detect the SAN upstroke of the OAPs using 2 different optical mapping systems (photodiode array and Ultima-L CMOS camera) with different spatial resolutions (up to 300×300 $\mu m^2$ per pixel) in conjunction with the use of 2 different voltage-sensitive dyes (di-4-ANNEPSs or RH237). Moreover, in some experiments, we detect clear SAN potentials in the absence atrial signals during exit-block induced by atrial pacing (Figures 2 and 4). The amplitude of the actual optical SAN signal varied from experiment to experiment and was dependent on the (1) optical mapping system, (2) the available spatial resolution, (3) the voltage-sensitive dyes and light sources, and (4) the anatomy of the SAN (Figure 1).
2. As shown by different groups,[14,16,31,102] including ours,[12,38] the dog and human SAN are located closer to epicardium near the superior vena cava ("head") and closer to endocardium near the inferior "tail" (Figures 1 and 3). Often, we observed the SAN upstroke component from only one side. In some cases, it was necessary to optically image from both sides to accurately visualize the activity of the SAN and calculate the CT (table I in the online data supplement of our study[12]). This method, however, was not included in the epicardial study by Joung et al.[13]
3. The interpretation of optical signals as reported in the study by Joung et al[13] study are based on the assumption that optical signals represent the morphology of a single SAN cell. We find this interpretation inappropriate, because microelectrode recordings published from the rabbit and canine SANs have never presented APs with multiphasic morphology found by both groups, except for single cases of electrotonic interaction near the line of block at the septal border of SAN (see figure 8 from the study by Bleeker et al 1980[26] and figure 8C from the study by Bromberg et al 1995[29]). Drs Joung and Lin now have found the second component of OAP near the septal margin of the SAN (Figure 8B) and thus confirm our rabbit[23,27] and canine[12] optical mapping studies. Our

Figures 3A and 4B clearly show an additional component of the OAP upstroke in the area of the canine septal block zone. Figure 4D shows that signals from the septal edge of SAN can contain all 3 components: SAN upstroke, atrial CT, and septal block zone (red arrow) upstrokes.

4. Because of their limited approach, the interpretation of optical signal maps presented by Joung et al[13] do not include SAN activation because activation time detected at 50% OAP amplitude represents only atrial muscle activation (the second component). This method does not detect preceding SAN activation, which, in nearly all cases, is relatively much smaller than the first component of optical recordings. As we reviewed above, numerous studies in many species have shown very slow conduction velocity within the SAN of 1 to 10 cm/sec. Maps in the study by Joung et al[13] showed very high conduction velocity, which is found only in the atrial myocardium.
5. The literature shows a significant delay from 30 up to 100 ms,[29] between the earliest activation of SAN and the earliest excitation of the atrial tissue (sinoatrial conduction time [SACT]). This does not agree with the interpretation of Joung et al,[13] who show this delay to be only ≈10ms. Moreover, the initial activation site in presented maps appears to coincide with breakthrough points, observed by many groups and does not project to anatomically defined SAN. This again suggests that the SAN activation was missed and only atrial activation was mapped. In figure 1 of our study,[12] we showed such a pattern of atrial activation at the epicardium and endocardium that deliberately ignores the separation of the 2 components and, therefore, misses the SAN.
6. Similarly, in our opinion, calcium optical signals from canine SAN should also contain multiple components corresponding to appropriate voltage signals. We do agree that LCRs (local subsarcolemmal ryanodine receptor-mediated $Ca^{2+}$ releases) may indeed facilitate SAN upstroke excitation as was shown by Vinogradova et al[55] from single rabbit SAN cells. Their shown stochastic but roughly periodic LCRs during the late phase of DD in rabbit sinoatrial nodal pacemaker cells generate an inward current ($I_{NCX}$) via the $Na^+/Ca^{2+}$ exchanger.[103] Thus, LCRs should be recorded during diastolic depolarization and not during the upstroke of SAN AP. In a new series of experiments (Figure 4), we used the same optical system (dual Ultima-L CMOS cameras) and the same voltage and calcium dyes that Joung et al used.[13] We could record double upstroke optical signals and presented individual activation patterns for both SAN and atrial layers. However, we were unable to confidently detect LCRs. It is our opinion, based on our experience, that the LCRs or LDCAEs recorded by Joung et al were the first component of SAN calcium upstroke. In our experiments, the calcium SAN upstroke always followed 7 to 20 ms after the voltage SAN upstroke at all recordings sites. We believe the LCRs in the study by Joung et al[13] are, in fact, optical recordings of intracellular calcium from the SAN, which precedes the much larger calcium signal from the atrial muscle and suggest that because of its low amplitude and stochastic behavior, the actual LCRs as noted by Vinogradova et al[55] would be difficult to record from intact canine SAN. To resolve this issue, we recommend that the same experiments be conducted on rabbits SAN instead of dogs, because the 2D structure of the rabbit SAN as compared to the 3D structure of the canine SAN.
7. Both groups have used the new electromechanical-uncoupler blebbistatin 10 to 20 μmol/L to eliminate motion artifact from optical recordings.[104] Joung et al showed that isoproterenol infusion (1 μmol/L) increased the sinus rate and noted the concomitant appearance of LDCAE preceding the AP upstroke by 98±31 ms. We conducted 5 canine SAN experiments in which we used Isoproterenol 1 μmol/L. We found that doses up to 20 μmol/L blebbistatin did not eliminate motion artifacts which significantly changed the morphology of the OAPs and thus hampered data analysis. Thus, the interpretation of the complex SAN OAPs during isoproterenol infusion has to be considered with caution because of the presence of motion artifact.
8. Finally, during work on this point–counterpoint, our opponents have agreed that the optical signals from the canine SAN region contain multiple components, which relate to the activation of different tissue layers because of both scattering and electrotonic effects. Figure 5 demonstrates the isochronal maps of the SAN DD and LDCAE by using nearly identical analytic approaches to those used in our study (see Figure 3).[12] Drs Joung and Lin used 50% of the "DD amplitude" to define SAN excitation (Figure 7B). The SAN activation maps (Figure 5E) and SACT (70.4±8.8 ms in 19 normal dogs) were determined based on this definition. However, this interpretation contradicts the classical definition of diastole and systole, which are separated by excitation. Therefore, excitation cannot happen during diastolic depolarization but only after it. For example, we adhere to the classic studies by Sano and Yamagishi[22] and Bleeker et al[26] that reconstruct SAN activation: (1) "*To estimate the arrival time of the excitation wave at each point, the steepest rise of the action potential of this point was used*" (see page 423[22]), or (2) "*As the activation moment of a cell, we chose the moment that the voltage was halfway between the maximal diastolic potential and the top of the action potential*" (see page 12[26]).

DD cannot be considered as pacemaker cell excitation because excitation is defined by the upstroke of AP. The phase of "fast" (according to Joung and Lin) diastolic depolarization in optical traces from the SAN actually contains both slow diastolic depolarization, as well as the upstroke of pacemaker AP, which can be separated for analysis (seen in optical recordings from the leading pacemaker in Figure 3A). We respectfully suggest Drs Joung and Lin to redefine the abbreviation "DD" for this part of SAN optical traces as SAN excitation time, as was done in the study by Fedorov et al.[12]

In conclusion, our first optical mapping studies focused on structure/function study at the tissue structure level. At this point, macroimaging cannot provide detailed insights into the ionic mechanisms of SAN pacemaker activity because to do so would require an isolated cell approach. However, we believe that after careful validation of SAN optical mapping methodology, optical mapping techniques could be applied to study the ionic mechanisms of pacemaker activity.

We hope that this rebuttal will benefit not only our 2 groups but will serve as a warning to all investigators using optical mapping techniques to study electrophysiology. Interpretation of the optically recorded APs can lead to radically different conclusions.

## Part IV. Boyoung Joung and Shien-Fong Lin Rebuttal

We fully agree that the macroscopic optical mapping collects light from the underlying 3D tissue. There is also no doubt that optical recording represents a weighted average of the depth signals. However, it is a significant challenge to assign correct weights to all the signal sources, especially when the sources are distributed rather than discrete entities. The tilted SAN structure in the transmural region and the dynamic shift of the dominant pacemaking site further complicate the weight assignment. Fedorov and Efimov model the SAN region with 2 tissue layers of equal weights. Such a simple approach may be sufficient to separate SAN and RA activations at the mid-SAN region in normal tissue, but the approach has only limited utility because of the strict requirements of signal shape and quality. As a result, their present method may be more suitable for confirming previous observations in normal tissue than for discovering new aspects such as automaticity and conduction in diseased tissue.

The opponents pointed out a wide variety of variability in their results that made their interpretation lack cohesion. For example, they indicated that the double potential is not always identifiable from a single side of the tissue. The reason for such an inconsistency is unclear. They also revealed that the amplitude of the optical SAN signal varied between experiments, and the first component is not always smaller than the second component. When the first component has larger amplitude than the second one, the second component is either buried in the first one or inseparable from the first. Fedorov and Efimov attributed these variable observations to SAN anatomy, but the structural variation causing the electrophysiological variance is not shown in their conceptual cartoon in Figure 3C. Furthermore, we consider the most significant limitation of their derivative approach is the inability to functionally identify the SAN boundary, where the first component diminishes in amplitude and falls below the detection threshold. As a result, the SAN region detected by signal analysis consistently underestimates the size of the SAN, and the localization of the exit sites becomes dubious.

We recorded $Ca_i$ and $V_m$ simultaneously in intact canine SAN. Our objective was to detect the interaction of $V_m$ and $Ca_i$ automaticity under normal condition and under accelerated heart rate during $\beta$-stimulation. Because of the lack of distinctive multiple components in the optical potentials, we used a straightforward interpretation of $Ca_i$ and $V_m$ tracings. Because there was no published method to measure the $Ca_i$ dynamics in SAN, we developed some new methods for data analysis. To locate the dominant pacemaker as precisely as possible, we used 4 published criteria.[22,26,29,89–92] Most importantly, the earliest activation site with fast diastolic depolarization colocalized with the site with the fastest LDACE elevation (Figure 6B, b). Based on such an observation, we concluded that Ca clock plays an important role in heart rate acceleration.

We did not attempt to resolve the depth issue in our previous study and did not plot the activation map inside the SAN.[13] The 50% activation level of optical potentials for the determination of activation isochrones in our study would represent the activation in the RA, because the level of DD never reached the 50% level of the amplitude. Compared to the opponents' new data in Figure 4, it is obvious that what we referred to as the DD was regarded as the SAN components by the opponents. Whereas the RA activation isochrones show the earliest RA activation (breakthrough site), the SAN DD and LDCAE maps clearly show the leading pacemaker site in the SAN. We think the "classical" approach of using 50% of the SAN upstroke for SAN activation would miss the opportunity to identify calcium release events preceding the phase 0. In our previous study, we did not present the data of SACT. The baseline SACT was calculated to be $70.4 \pm 8.8$ ms in 19 normal dogs.[87]

In addition to the opponents' historical perspective, many recent studies from multiple investigators showed that the SR calcium release is also an important mechanism of SAN automaticity.[48–59] These publications document that the spontaneous and rhythmic SR Ca release works synergistically with membrane ion clock to generate SAN automaticity. Therefore, a complete functional study of SAN should include not only optical mapping of the membrane potential changes but also optical mapping of the dynamic changes of intracellular calcium concentration. What we were studying was the events that occurred before the onset of the sinus node or atrial APs. On the other hand, our opponents' results depend heavily on the analysis of the phase 0 of the AP both in the SAN and the atrium. Specifically, our results, as well as that reported by many other investigators, were based primarily on the events that happened to late phase of the AP. Because the sinus node alone has significant spontaneous phase 4 depolarization, the diastolic depolarization and the LDCAE were changes unique to the sinus node.

Fedorov and Efimov show new, unpublished data obtained from the high-resolution CMOS cameras (Figure 4). The new data reveal a few interesting aspects supporting that the optical system indeed plays a role in data acquisition. Most importantly, the quality of optical potentials traces and activation isochrones degrades with the increased spatial resolution. This is likely attributable to less spatial averaging of each physical pixel during imaging and the lack of interpixel interpolation during the construction of isochrones. The double-component morphology in the optical potential (Figure 4B) is much less obvious in this new setup with smaller pixels size. It will be a challenge to clearly separate the DD, SAN, and RA component in this new data set. Consistent with our results, Fedorov and Efimov did not find LDCAE in the baseline condition without $\beta$-stimulation. Their ability to record $V_m$ and $Ca_i$ from the SAN in the pacing-induced exit block case (Figure 4D) offers a unique way to independently observe SAN activation. However, the long-term pacing of 10 minutes could alter the SAN physiology and the following activation could come from ectopic origins. Furthermore, ryanodine has only modest effects on

sinus rate in intact SAN in baseline conditions[13,66] but is highly effective in preventing sinus rate acceleration during isoproterenol infusion. Their results, which show ryanodine had no significant effects on sinus rate at baseline, is not consistent with those reports. Nevertheless, we predict that their preparations pretreated with ryanodine would not be able to effectively respond to $\beta$-stimulation.

We want to emphasize that it is important to incorporate the study of intracellular calcium in optical mapping studies of the sinoatrial node and other cardiac structures that exhibit rhythmic behavior. Without such information, it is not possible to understand how sinoatrial node in specific or cardiac automaticity in general works in intact hearts. In the meantime, it is essential to carefully improve the acquisition technique and signal analysis approach to more accurately resolve the depth issue in optical mapping. These combined efforts will lead to new findings in addition to supporting existing models.

## Acknowledgments

We thank Dr Peng-Sheng Chen for his review and comments.

## Sources of Funding

Supported, in part, by NIH grants P01 HL78931, R01 HL78932, and 71140 and an American Heart Association Established Investigator Award (to S.F.L.); American Heat Association Beginning-Grant-In-Aid 0860047Z (to V.V.F.); and NIH grant R01 HL085369 (to I.R.E.).

## Disclosures

None.

## References

1. Keith A, Flack M. The form and nature of the muscular connection between the primary divisions of the vertebrate heart. *J Anat Physiol*. 1907;41:172–189.
2. Tawara S. *Das Reizleitungssystem des Saugetierherzens: Eine Anatomische-Histologische Studie Uber Das Atrioventrikularbundel Und Die Purkinjeschen Faden*. 1906. Jena, Germany: Verlag von Gustav Fischer.
3. Lewis T, Oppenheimer A, Oppenheimer BS. The site of origin of the mammalian heart beat: the pacemaker in the dog. *Heart.* 1910;II: 147–169.
4. Wybauw. *Archives Internationales de Physiologie.* 1910;x:78.
5. Mangoni ME, Nargeot J. Genesis and regulation of the heart automaticity. *Physiol Rev*. 2008;88:919–982.
6. Lakatta EG, DiFrancesco D. What keeps us ticking: a funny current, a calcium clock, or both? *J Mol Cell Cardiol*. 2009;47:157–170.
7. Rosen MR. 15th annual Gordon K. Moe Lecture. Biological pacemaking: in our lifetime? *Heart Rhythm*. 2005;2:418–428.
8. Efimov IR, Nikolski VP, Salama G. Optical imaging of the heart. *Circ Res*. 2004;95:21–33.
9. Baxter WT, Mironov SF, Zaitsev AV, Jalife J, Pertsov AM. Visualizing excitation waves inside cardiac muscle using transillumination. *Biophys J*. 2001;80:516–530.
10. Bray MA, Wikswo JP. Examination of optical depth effects on fluorescence imaging of cardiac propagation. *Biophys J*. 2003;85:4134–4145.
11. Bishop MJ, Rodriguez B, Qu F, Efimov IR, Gavaghan DJ, Trayanova NA. The role of photon scattering in optical signal distortion during arrhythmia and defibrillation. *Biophys J*. 2007;93:3714–3726.
12. Fedorov VV, Schuessler RB, Hemphill M, Ambrosi CM, Chang R, Voloshina AS, Brown K, Hucker WJ, Efimov IR. Structural and functional evidence for discrete exit pathways that connect the canine sinoatrial node and atria. *Circ Res*. 2009;104:915–923.
13. Joung B, Tang L, Maruyama M, Han S, Chen Z, Stucky M, Jones LR, Fishbein MC, Weiss JN, Chen PS, Lin SF. Intracellular calcium dynamics and acceleration of sinus rhythm by beta-adrenergic stimulation. *Circulation*. 2009;119:788–796.
14. James TN. Anatomy of the human sinus node. *Anat Rec*. 1961;141: 109–139.
15. James TN. Structure and function of the sinus node, AV node and His bundle of the human heart: part I-structure. *Prog Cardiovasc Dis*. 2002;45:235–267.
16. Truex RC, Smythe MQ, Taylor MJ. Reconstruction of the human sinoatrial node. *Anat Rec*. 1967;159:371–378.
17. James T. The connecting pathways between the sinus node and the A-V node and between the right and left atrium of the human heart. *Am Heart J*. 1963;66:498–508.
18. Eyster JAE, Meek WJ. Experiments on the origin and propagation of the impulse in the heart: point of primary negativity in the mammalian heart and the spread of negativity to other regions. *Heart*. 1913;5:119–136.
19. Meek WJ, Eyster JAE. The effect of vagal stimulation and of colling on the location of the pacemaker within the sino-auricular node. *Am J Physiol*. 1914;34:368–383.
20. Trautwein W, Zink K. [Membrane and action potentials of single myocardial fibers of cold and warmblooded animals.]. *Pflugers Arch.* 1952; 256:64–84.
21. de Carvalho AP, de Mello WC, Hoffman BF. Electrophysiological evidence for specialized fiber types in rabbit atrium. *Am J Physiol*. 1959;196:483–488.
22. Sano T, Yamagishi S. Spread of excitation from the sinus node. *Circ Res*. 1965;16:423–430.
23. Efimov IR, Fahy GJ, Cheng YN, Van Wagoner DR, Tchou PJ, Mazgalev TN. High resolution fluorescent imaging of rabbit heart does not reveal a distinct atrioventricular nodal anterior input channel (fast pathway) during sinus rhythm. *J Cardiovasc Electrophysiol*. 1997;8: 295–306.
24. Boyett MR, Honjo H, Yamamoto M, Nikmaram MR, Niwa R, Kodama I. Downward gradient in action potential duration along conduction path in and around the sinoatrial node. *Am J Physiol*. 1999;276:H686–H698.
25. Vinogradova TM, Fedorov VV, Yuzyuk TN, Zaitsev AV, Rosenshtraukh LV. Local cholinergic suppression of pacemaker activity in the rabbit sinoatrial node. *J Cardiovasc Pharmacol*. 1998;32:413–424.
26. Bleeker WK, Mackaay AJ, Masson-Pevet M, Bouman LN, Becker AE. Functional and morphological organization of the rabbit sinus node. *Circ Res*. 1980;46:11–22.
27. Fedorov VV, Hucker WJ, Dobrzynski H, Rosenshtraukh LV, Efimov IR. Postganglionic Nerve Stimulation Induces Temporal Inhibition of Excitability in the Rabbit Sinoatrial Node. *Am J Physiol*. 2006;291: H612–H623.
28. Shibata N, Inada S, Mitsui K, Honjo H, Yamamoto M, Niwa R, Boyett MR, Kodama I. Pacemaker shift in the rabbit sinoatrial node in response to vagal nerve stimulation. *Exp Physiol*. 2001;86:177–184.
29. Bromberg BI, Hand DE, Schuessler RB, Boineau JP. Primary negativity does not predict dominant pacemaker location: implications for sinoatrial conduction. *Am J Physiol*. 1995;269:H877–H887.
30. Kwong KF, Schuessler RB, Green KG, Laing JG, Beyer EC, Boineau JP, Saffitz JE. Differential expression of gap junction proteins in the canine sinus node. *Circ Res*. 1998;82:604–612.
31. James TN. Anatomy of the sinus node of the dog. *Anat Rec*. 1962;143: 251–265.
32. Boineau JP, Canavan TE, Schuessler RB, Cain ME, Corr PB, Cox JL. Demonstration of a widely distributed atrial pacemaker complex in the human heart. *Circulation*. 1988;77:1221–1237.
33. Verkerk AO, van Ginneken AC, Wilders R. Pacemaker activity of the human sinoatrial node: role of the hyperpolarization-activated current, I (f). *Int J Cardiol.* 2009;132:318–336.
34. Schuessler RB. Abnormal sinus node function in clinical arrhythmias. *J Cardiovasc Electrophysiol*. 2003;14:215–217.
35. Durrer D, Dam RTv, Freud GE, Janse MJ, Meijler FL, Arzbaecher RC. Total excitation of the isolated human heart. *Circulation*. 1970;41: 899–912.
36. Cosio FG, Martin-Penato A, Pastor A, Nunez A, Montero MA, Cantale CP, Schames S. Atrial activation mapping in sinus rhythm in the clinical electrophysiology laboratory: observations during Bachmann's bundle block. *J Cardiovasc Electrophysiol.* 2004;15:524–531.
37. Boineau JP, Schuessler RB, Mooney CR, Wylds AC, Miller CB, Hudson RD, Borremans JM, Brockus CW. Multicentric origin of the atrial depolarization wave: the pacemaker complex. Relation to dynamics of atrial conduction, P-wave changes and heart rate control. *Circulation*. 1978;58:1036–1048.

38. Fedorov VV, Glukhov AV, Chang R, Kostecki G, Alferol H, Wuskell J, Loew LM, Moazami N, Efimov IR. The origin of heartbeat in the human sinus node: evidence of sino-atrial exit pathways. *Circulation.* 2009;119.
39. Tuchin V. Tissue optics: light scattering methods and instruments for medical diagnosis. Bellingham, Wash: SPIE Press; 2007.
40. Efimov IR, Mazgalev TN. High-resolution three-dimensional fluorescent imaging reveals multilayer conduction pattern in the atrioventricular node. *Circulation*. 1998;98:54–57.
41. Efimov IR, Sidorov VY, Cheng Y, Wollenzier B. Evidence of 3D scroll waves with ribbon-shaped filament as a mechanism of ventricular tachycardia in the isolated rabbit heart. *J Cardiovasc Electrophysiol*. 1999;10:1452–1462.
42. Janks DL, Roth BJ. Averaging over depth during optical mapping of unipolar stimulation. *IEEE Trans Biomed Eng*. 2002;49:1051–1054.
43. Nikolski V, Efimov I. Fluorescent imaging of a dual-pathway atrioventricular-nodal conduction system. *Circ Res*. 2001;88:e23–e30.
44. Hyatt CJ, Mironov SF, Vetter FJ, Zemlin CW, Pertsov AM. Optical action potential upstroke morphology reveals near-surface transmural propagation direction. *Circ Res*. 2005;97:277–284.
45. Toda N, Shimamoto K. The influence of sympathetic stimulation on transmembrane potentials in the S-A node. *J Pharmacol Exp Ther*. 1968;159:298–305.
46. Brown HF, DiFrancesco D, Noble SJ. How does adrenaline accelerate the heart? *Nature*. 1979;280:235–236.
47. Baruscotti M, Bucchi A, DiFrancesco D. Physiology and pharmacology of the cardiac pacemaker ("funny") current. *Pharmacol Ther*. 2005;107:59–79.
48. Rubenstein DS, Lipsius SL. Mechanisms of automaticity in subsidiary pacemakers from cat right atrium. *Circ Res*. 1989;64:648–657.
49. Hata T, Noda T, Nishimura M, Watanabe Y. The role of Ca2+ release from sarcoplasmic reticulum in the regulation of sinoatrial node automaticity. *Heart Vessels*. 1996;11:234–241.
50. Zhou Z, Lipsius SL. Na(+)-Ca2+ exchange current in latent pacemaker cells isolated from cat right atrium. *J Physiol*. 1993;466:263–285.
51. Rigg L, Terrar DA. Possible role of calcium release from the sarcoplasmic reticulum in pacemaking in guinea-pig sino-atrial node. *Exp Physiol*. 1996;81:877–880.
52. Li J, Qu J, Nathan RD. Ionic basis of ryanodine's negative chronotropic effect on pacemaker cells isolated from the sinoatrial node. *Am J Physiol*. 1997;273:H2481–H2489.
53. Ju YK, Allen DG. Intracellular calcium and Na+-Ca2+ exchange current in isolated toad pacemaker cells. *J Physiol*. 1998;508(pt 1):153–166.
54. Huser J, Blatter LA, Lipsius SL. Intracellular Ca2+ release contributes to automaticity in cat atrial pacemaker cells. *J Physiol.* 2000;524(pt 2):415–422.
55. Vinogradova TM, Bogdanov KY, Lakatta EG. beta-Adrenergic stimulation modulates ryanodine receptor Ca(2+) release during diastolic depolarization to accelerate pacemaker activity in rabbit sinoatrial nodal cells. *Circ Res*. 2002;90:73–79.
56. Vinogradova TM, Bogdanov KY, Lakatta EG. Novel perspectives on the beating rate of the heart. *Circ Res*. 2002;91:e3.
57. Bogdanov KY, Vinogradova TM, Lakatta EG. Sinoatrial nodal cell ryanodine receptor and Na(+)-Ca(2+) exchanger: molecular partners in pacemaker regulation. *Circ Res*. 2001;88:1254–1258.
58. Maltsev VA, Vinogradova TM, Lakatta EG. The emergence of a general theory of the initiation and strength of the heartbeat. *J Pharmacol Sci*. 2006;100:338–369.
59. Vinogradova TM, Lyashkov AE, Zhu W, Ruknudin AM, Sirenko S, Yang D, Deo S, Barlow M, Johnson S, Caffrey JL, Zhou YY, Xiao RP, Cheng H, Stern MD, Maltsev VA, Lakatta EG. High basal protein kinase A-dependent phosphorylation drives rhythmic internal Ca2+ store oscillations and spontaneous beating of cardiac pacemaker cells. *Circ Res*. 2006;98:505–514.
60. Verheijck EE, van Kempen MJ, Veereschild M, Lurvink J, Jongsma HJ, Bouman LN. Electrophysiological features of the mouse sinoatrial node in relation to connexin distribution. *Cardiovasc Res*. 2001;52:40–50.
61. Lei M, Jones SA, Liu J, Lancaster MK, Fung SS, Dobrzynski H, Camelliti P, Maier SK, Noble D, Boyett MR. Requirement of neuronal- and cardiac-type sodium channels for murine sinoatrial node pacemaking. *J Physiol*. 2004;559:835–848.
62. Lancaster MK, Jones SA, Harrison SM, Boyett MR. Intracellular Ca2+ and pacemaking within the rabbit sinoatrial node: heterogeneity of role and control. *J Physiol*. 2004;556:481–494.
63. Tellez JO, Dobrzynski H, Greener ID, Graham GM, Laing E, Honjo H, Hubbard SJ, Boyett MR, Billeter R. Differential expression of ion channel transcripts in atrial muscle and sinoatrial node in rabbit. *Circ Res*. 2006;99:1384–1393.
64. Boineau JP, Miller CB, Schuessler RB, Roeske WR, Autry LJ, Wylds AC, Hill DA. Activation sequence and potential distribution maps demonstrating multicentric atrial impulse origin in dogs. *Circ Res*. 1984;54:332–347.
65. Schuessler RB, Boineau JP, Wylds AC, Hill DA, Miller CB, Roeske WR. Effect of canine cardiac nerves on heart rate, rhythm, and pacemaker location. *Am J Physiol*. 1986;250:H630–H644.
66. Honjo H, Inada S, Lancaster MK, Yamamoto M, Niwa R, Jones SA, Shibata N, Mitsui K, Horiuchi T, Kamiya K, Kodama I, Boyett MR. Sarcoplasmic reticulum Ca2+ release is not a dominating factor in sinoatrial node pacemaker activity. *Circ Res*. 2003;92:e41–e44.
67. Nikmaram MR, Boyett MR, Kodama I, Suzuki R, Honjo H. Variation in effects of Cs+, UL-FS-49, and ZD-7288 within sinoatrial node. *Am J Physiol*. 1997;272:H2782–H2792.
68. Leitch SP, Sears CE, Brown HF, Paterson DJ. Effects of high potassium and the bradycardic agents ZD7288 and cesium on heart rate of rabbits and guinea pigs. *J Cardiovasc Pharmacol*. 1995;25:300–306.
69. Denyer JC, Brown HF. Pacemaking in rabbit isolated sino-atrial node cells during Cs+ block of the hyperpolarization-activated current if. *J Physiol*. 1990;429:401–409.
70. Joung B, Tang L, Han S, Maruyama M, Chen PS, Lin SF. Cellular mechanism underlying sick sinus syndromes in intact canine sinoatrial node. *J Am Coll Cardio*. 2009;53:A102.
71. Dobrzynski H, Boyett MR, Anderson RH. New insights into pacemaker activity: promoting understanding of sick sinus syndrome. *Circulation*. 2007;115:1921–1932.
72. Jones SA, Lancaster MK, Boyett MR. Ageing-related changes of connexins and conduction within the sinoatrial node. *J Physiol*. 2004;560:429–437.
73. Jones SA, Boyett MR, Lancaster MK. Declining into failure: the age-dependent loss of the L-type calcium channel within the sinoatrial node. *Circulation*. 2007;115:1183–1190.
74. Verkerk AO, Wilders R, Coronel R, Ravesloot JH, Verheijck EE. Ionic remodeling of sinoatrial node cells by heart failure. *Circulation*. 2003;108:760–766.
75. Sanders P, Kistler PM, Morton JB, Spence SJ, Kalman JM. Remodeling of sinus node function in patients with congestive heart failure: reduction in sinus node reserve. *Circulation*. 2004;110:897–903.
76. Elvan A, Wylie K, Zipes DP. Pacing-induced chronic atrial fibrillation impairs sinus node function in dogs. Electrophysiological remodeling. *Circulation*. 1996;94:2953–2960.
77. Hocini M, Sanders P, Deisenhofer I, Jais P, Hsu LF, Scavee C, Weerasoriya R, Raybaud F, Macle L, Shah DC, Garrigue S, Le Metayer P, Clementy J, Haissaguerre M. Reverse remodeling of sinus node function after catheter ablation of atrial fibrillation in patients with prolonged sinus pauses. *Circulation*. 2003;108:1172–1175.
78. Benson DW, Wang DW, Dyment M, Knilans TK, Fish FA, Strieper MJ, Rhodes TH, George AL Jr. Congenital sick sinus syndrome caused by recessive mutations in the cardiac sodium channel gene (SCN5A). *J Clin Invest*. 2003;112:1019–1028.
79. Veldkamp MW, Wilders R, Baartscheer A, Zegers JG, Bezzina CR, Wilde AA. Contribution of sodium channel mutations to bradycardia and sinus node dysfunction in LQT3 families. *Circ Res*. 2003;92:976–983.
80. Milanesi R, Baruscotti M, Gnecchi-Ruscone T, DiFrancesco D. Familial sinus bradycardia associated with a mutation in the cardiac pacemaker channel. *N Engl J Med*. 2006;354:151–157.
81. Mohler PJ, Bennett V. Ankyrin-based cardiac arrhythmias: a new class of channelopathies due to loss of cellular targeting. *Curr Opin Cardiol*. 2005;20:189–193.
82. Bhuiyan ZA, Van Den Berg MP, van Tintelen JP, Bink-Boelkens MT, Wiesfeld AC, Alders M, Postma AV, van LI, Mannens MM, Wilde AA. Expanding spectrum of human RYR2-related disease: new electrocardiographic, structural, and genetic features. *Circulation*. 2007;116:1569–1576.
83. Ogawa M, Zhou S, Tan AY, Song J, Gholmieh G, Fishbein MC, Luo H, Siegel RJ, Karagueuzian HS, Chen LS, Lin SF, Chen PS. Left stellate ganglion and vagal nerve activity and cardiac arrhythmias in ambulatory dogs with pacing-induced congestive heart failure. *J Am Coll Cardiol*. 2007;50:335–343.

84. Lakatta EG, Maltsev VA, Bogdanov KY, Stern MD, Vinogradova TM. Cyclic variation of intracellular calcium: a critical factor for cardiac pacemaker cell dominance. *Circ Res*. 2003;92:e45–e50.
85. Yeh YH, Burstein B, Qi XY, Sakabe M, Chartier D, Comtois P, Wang Z, Kuo CT, Nattel S. Funny current downregulation and sinus node dysfunction associated with atrial tachyarrhythmia: a molecular basis for tachycardia-bradycardia syndrome. *Circulation*. 2009;119:1576–1585.
86. Zicha S, Fernandez-Velasco M, Lonardo G, L'Heureux N, Nattel S. Sinus node dysfunction and hyperpolarization-activated (HCN) channel subunit remodeling in a canine heart failure model. *Cardiovasc Res*. 2005;66:472–481.
87. Joung B, Lin S-F, Chen Z, Antoun PS, Maruyama M, Han S, Piccirillo G, Stucky M, Zipes DP, Chen PS, Das MK. Mechanisms of sinoatrial node dysfunction in a canine model of pacing-induced atrial fibrillation. *Heart Rhythm.* September 16, 2009 [Epub ahead of print] PMID: 19914141.
88. Maltsev VA, Lakatta EG. Synergism of coupled subsarcolemmal Ca2+ clocks and sarcolemmal voltage clocks confers robust and flexible pacemaker function in a novel pacemaker cell model. *Am J Physiol Heart Circ Physiol*. 2009;296:H594–H615.
89. West TC. Ultramicroelectrode recording from the cardiac pacemaker. *J Pharmacol Exp Ther*. 1955;115:283–290.
90. de Carvalho AP, de Mello WC, Hoffman BF, eds. *The Specialized Tissues of the Heart*. Amsterdam, The Netherlands: Elsevier; 1961.
91. Kohlhardt M, Figulla HR, Tripathi O. The slow membrane channel as the predominant mediator of the excitation process of the sinoatrial pacemaker cell. *Basic Res Cardiol*. 1976;71:17–26.
92. Seyama I. Characteristics of the rectifying properties of the sino-atrial node cell of the rabbit. *J Physiol*. 1976;255:379–397.
93. James TN. Structure and function of the sinus node, AV node and his bundle of the human heart: part II–function. *Prog Cardiovasc Dis*. 2003;45:327–360.
94. Woods WT, Urthaler F, James TN. Spontaneous action potentials of cells in the canine sinus node. *Circ Res*. 1976;39:76–82.
95. Wiedmann RT, Tan RC, Joyner RW. Discontinuous conduction at Purkinje-ventricular muscle junction. *Am J Physiol*. 1996;271:H1507–H1516.
96. Bishop MJ, Bub G, Garny A, Gavaghan DJ, Rodriguez B. An investigation into the role of the optical detection set-up in the recording of cardiac optical mapping signals: A Monte Carlo simulation study. *Physica D*. 2009;238:1008–1018.
97. Bien H, Parikh P, Entcheva E. Lenses and effective spatial resolution in macroscopic optical mapping. *Phys Med Biol*. 2007;52:941–960.
98. Sedmera D, Reckova M, Rosengarten C, Torres MI, Gourdie RG, Thompson RP. Optical mapping of electrical activation in the developing heart. *Microsc Microanal*. 2005;11:209–215.
99. Danik SB, Rosner G, Lader J, Gutstein DE, Fishman GI, Morley GE. Electrical remodeling contributes to complex tachyarrhythmias in connexin43-deficient mouse hearts. *FASEB J*. 2008;22:1204-1212.
100. Morley GE, Vaidya D. Understanding conduction of electrical impulses in the mouse heart using high-resolution video imaging technology. *Microsc Res Tech*. 2001;52:241–250.
101. de Diego C, Chen F, Xie LH, Dave AS, Thu M, Rongey C, Weiss JN, Valderrabano M. Cardiac alternans in embryonic mouse ventricles. *Am J Physiol Heart Circ Physiol*. 2008;294:H433–H440.
102. Chandler NJ, Greener ID, Tellez JO, Inada S, Musa H, Molenaar P, DiFrancesco D, Baruscotti M, Longhi R, Anderson RH, Billeter R, Sharma V, Sigg DC, Boyett MR, Dobrzynski H. Molecular architecture of the human sinus node: insights into the function of the cardiac pacemaker. *Circulation*. 2009;119:1562–1575.
103. Bogdanov KY, Maltsev VA, Vinogradova TM, Lyashkov AE, Spurgeon HA, Stern MD, Lakatta EG. Membrane potential fluctuations resulting from submembrane Ca2+ releases in rabbit sinoatrial nodal cells impart an exponential phase to the late diastolic depolarization that controls their chronotropic state. *Circ Res*. 2006;99:979–987.
104. Fedorov VV, Lozinsky IT, Sosunov EA, Anyukhovsky EP, Rosen MR, Balke CW, Efimov IR. Application of blebbistatin as an excitation-contraction uncoupler for electrophysiologic study of rat and rabbit hearts. *Heart Rhythm*. 2007;4:619–626.